Synthesis and Properties of $[Ru_2(acac)_4(bptz)]^{n+}$ ($n = 0, 1$) and Crystal Structure of $[Ru_2(acac)_4(bptz)]$

Sudha Chellamma and Marya Lieberman*

Department of Chemistry and Biochemistry, University of Notre Dame, Notre Dame, Indiana 46556

Received December 6, 2000

The neutral complex $[Ru_2(acac)_4(bptz)]$ (**I**) has been prepared by the reaction of $Ru(acac)_2(CH_3CN)_2$ with bptz (bptz = 3,6-bis(2-pyridyl)-1,2,4,5-tetrazine) in acetone. The diruthenium(II,II) complex (**I**) is green and exhibits an intense metal−ligand charge-transfer band at 700 nm. Complex **I** is diamagnetic and has been characterized by NMR, optical spectroscopy, IR, and single-crystal X-ray diffraction. Crystal structure data for **I** are as follows: triclinic, $P\bar{1}$, $a = 11.709(2)$ Å, $b = 13.487(3)$ Å, $c = 15.151(3)$ Å, $\alpha = 65.701(14)°$, $\beta = 70.610(14)°$, $\gamma = 75.50(2)°$, $V = 2038.8(6)$ Å^3, $Z = 2$, $R = 0.0610$, for 4397 reflections with $F_o > 4\sigma F_o$. Complex **I** shows reversible $Ru_2(II,II)-Ru_2(II,III)$ and $Ru_2(II,III)-Ru_2(III,III)$ couples at 0.17 and 0.97 V, respectively; the 800 mV separation indicates considerable stabilization of the mixed-valence species ($K_{com} > 10^{13}$). The diruthenium(II,III) complex, $[Ru_2(acac)_4(bptz)](PF_6)$ (**II**) is prepared quantitatively by one-electron oxidation of **I** with cerium(IV) ammonium nitrate in methanol followed by precipitation with NH_4PF_6. Complex **II** is blue and shows an intense MLCT band at 575 nm and a weak band at 1220 nm in $CHCl_3$, which is assigned as the intervalence CT band. The mixed valence complex is paramagnetic, and an isotropic EPR signal at $g = 2.17$ is observed at 77 and 4 K. The solvent independence and narrowness of the 1200 nm band show that complex **II** is a Robin and Day class III mixed-valence complex.

Introduction

Since the discovery of the Creutz−Taube (CT) ion, there have been scores of reports on diruthenium mixed-valence complexes.[1−4] Most of these complexes contain neutral bridging and supporting ligands, and hence, they are multiply charged. We are curious about how reduction of this net charge might affect charge transfer and other physical properties of mixed-valence compounds. Here, we report the synthesis, electrochemical properties, and crystal structure of the neutral ruthenium dimer $[Ru_2(acac)_4(bptz)]$ (**I**) (acac = acetylacetonate, bptz = 3,6-bis-(2-pyridyl)-1,2,4,5-tetrazine), as well as the synthesis and characterization of its monocationic oxidation product, $[Ru_2(acac)_4(bptz)](PF_6)$ (**II**).

The relatively high charge of most mixed-valence ruthenium complexes arises because the neutral supporting ligands, such as ammonia and 2,2′-bpy (bpy = bipyridyl), do not cancel out the charge on the ruthenium atoms. Species with cyanide supporting ligands are known,[5] but in these species the negative charge of four or five cyanides on each ruthenium overwhelms the metal charge to give polyanionic mixed-valence species. Mixtures of neutral and charged supporting ligands would overcome this problem, but might create other problems in synthesis and purification. Instead, we picked acac, a bidentate, uninegative ligand which would compensate for up to two positive charges per ruthenium cation. The π-acceptor ability of acac is weak, and acac is more comparable to ammonia rather than to a good π-acid like bpy or bptz.

In recent years, the bis-chelating 3,6-bis(2-pyridyl)-1,2,4,5-tetrazine (bptz) ligand has been used for the self-assembly of metal dimers[6−8] and tetramers.[9−10] Due to its σ donor/π acceptor character it provides very strong coupling between metal centers, at least as measured by the electrochemical separation between sucessive oxidations of the two metal centers.

Experimental Section

The preparation of **I** was carried out under a dry argon atmosphere, using standard Schlenk line and glovebox techniques. Acetone and dichloromethane were distilled prior to use, and other solvents were used without any further purification. *Cis*-$Ru(acac)_2(CH_3CN)_2$ was synthesized from $Ru(acac)_3$ (Aldrich) by Kobayashi's procedure.[11]

UV−Visible spectra were recorded with a Beckman DU-7500 spectrophotometer. Near-IR studies were carried out using a Lamda

* To whom correspondence should be addressed.

(1) Creutz, C. *Prog. Inorg. Chem.* **1983**, *30*, 1.
(2) (a) Creutz, C.; Taube, H. J. *Am. Chem. Soc.* **1969**, *91*, 3988. (b) Creutz, C.; Taube, H. *J. Am. Chem. Soc.* **1973**, *95*, 1086. (c) Richardson, D. E.; Taube, H. *J. Am. Chem. Soc.* **1983**, *105*, 40. (d) Richardson, D. E.; Taube, H. *Coord. Chem. Rev.* **1984**, *60*, 107. (e) Lay, P. A.; Magnuson, R. H.; Taube, H. *Inorg. Chem.* **1988**, *27*, 2364.
(3) (a) Tanner, M.; Ludi, A. *Inorg. Chem.* **1981**, *20*, 2348. (b) Callahan, R. W.; Keene, R.; Meyer, T. J.; Salmon, D. J. *J. Am. Chem. Soc.* **1977**, *99* 1064. (c) Kaim, W.; Klein, A.; Glockle, M. *Acc. Chem. Res.* **2000**, *33*, 755.
(4) Strekas, T. C.; Spiro, T. G. *Inorg. Chem.* **1976**, *15*, 974.
(5) Scheiring, T.; Kaim, W.; Olabe, J. A.; Parise, A. R.; Fiedler, J. *Inorg. Chim. Acta* **2000**, *301*, 125.
(6) (a) Schwach, M.; Hause, H.; Kaim, W. *Inorg. Chem.* **1999**, *38*, 2242. (b) Poppe, J.; Moscherosch, M.; Kaim, W. *Inorg. Chem.* **1993**, *32*, 2640. (c) Johnson, J. E. B.; de Groff, C.; Ruminski, R. R. *Inorg. Chim. Acta* **1991**, *187*, 73. (d) Kaim, W.; Kasack, V. *Inorg. Chem.* **1990**, *29*, 4696.
(7) Jaradadt, Q.; Barqawi, K.; Akasheh, T. S. *Inorg. Chim. Acta* **1986**, *116*, 63.
(8) Roche, S.; Yellowlees, L. J.; Thomas, J. A. *J. Chem. Soc., Chem. Commun.* **1998**, 1429.
(9) Campos-Fernandez, C. S.; Clerac, R.; Dunbar, K. M. *Ang. Chem., Int. Ed.* **1999**, *38*, 3477.
(10) Bu, H.; Morishita, H.; Tanaka, K.; Biradha, K.; Furusho, S.; Shinoya, M. *J. Chem. Soc., Chem. Commun.* **2000**, 971.
(11) Kobayashi, Y.; Nishina, Y.; Shimizu, K.; Sato, G. P. *Chem. Lett.* **1988**, 1137.

10.1021/ic001374w CCC: $20.00
Published on Web 05/22/2001

Table 1. Comparison of Electrochemical and Spectroscopic Data for **I** and Similar Complexes

complex	MLCT λ_{max} nm (ϵ, M^{-1} cm^{-1})	IVCT (solvent) λ_{max}, nm (ϵ, M^{-1} cm^{-1})	$(Ru^{II},Ru^{III})-(Ru_2^{II})$ (ΔE_p)	$(Ru^{II},Ru^{III})-(Ru_2^{III})$ (ΔE_p)	other potentials (ΔE_p)	K_C [f]	ref
I[a]	**707 (22000)**	–					**this work**
II	**575**	**CH_2Cl_2: 1217 (20)** **$CHCl_3$: 1219 (12)** **CH_3CN: 1238 (20)**	**0.17 (65)**	**0.97 (65)**	**−1.11 (80)[g]**	**10^{13}**	**this work**
$[Ru_2(NH_3)_8(bptz)]^{4+}$ [b]	603 (19000) (519 for Ru_2II,III)	1450	0.72 (65)	1.56 (90)	−1.49 (65)	10^{15}	6c
$[Ru_2(bpy)_4(bptz)]^{4+}$ [c]	683 (12000)		1.52 (60)	2.02 (70)	−0.70 (70) −1.25 (irr)	$10^{8.5}$	12b
$[Ru_2(bpy)_4(pz)Cl_2]^{2+}$ [d]	513 (26000)	1050	0.89 (80)	1.01 (80)	−0.03 (60) −	100	3b
$[(RuCl[9]aneS_3)_2bptz]$[d]	751 (2281) (678 for Ru_2II,III)	1852	1.3 (<100)	1.84 (<100)	−	10^8	8
$[Ru_2(NH_3)_{10}(pz)]^{4+}$ [e]	547 (30000)	1570	0.38 (65)	0.77 (80)	−	$10^{6.6}$	2e

[a] CH_2Cl_2-$TBABF_4$: E (V) vs Ag/AgCl. [b] CH_3CN-$TBAClO_4$: E (V) vs Ag/AgCl. [c] CH_3CN-$TBAClO_4$: E (V) vs SCE. [d] CH_3CN-$TBAPF_6$: E (V) vs SCE. [e] 0.1 M HCl: E vs. NHE [f] $Kc = 10^{\Delta E/0.059\ V}$; irr, irreversible. [g] Free bptz shows a reduction at −0.77 V (140 mV).

19 Perkin−Elmer spectrometer. ^1H NMR spectra were recorded on a Varian 300 NMR spectrometer; peak positions were referenced to solvent residuals. Mass spectra (FAB+) were recorded on a JEOL JMS-AX505HA mass spectrometer from a matrix of *p*-nitrobenzyl alcohol. Elemental analyses were obtained from MHW Laboratories, Phoenix, AZ. EPR spectra were recorded on a Bruker EMX X-band EPR spectrometer at 77 and 4 K.

Cyclic voltammetric measurements were performed using an EG & G PAR Potentiostat Model 283 whose wires were passed into an Innovative Technologies drybox with a nitrogen atmosphere. The working, counter, and reference electrodes were a platinum button, a platinum wire, and Ag/AgCl, respectively. Tetrabutylammonium tetrafluoroborate ($TBABF_4$) (0.1 M) was used as the supporting electrolyte, and the measurements were recorded at 25 °C. Ferrocene was used as an internal standard to verify the pseudo-reference potential; the Fe(II)/Fe(III) couple was observed at 0.52 V in CH_2Cl_2 against the Ag/AgCl pseudo-reference electrode.

Synthesis of $[Ru_2(acac)_4(bptz)]$ (I). $Ru(acac)_2(CH_3CN)_2$ (60 mg, 0.16 mmol) was dissolved in acetone (10 mL), and bptz (18.7 mg, 0.08 mmol) was added to the solution in the drybox. The reaction mixture was refluxed for 4 h under an argon atmosphere. A green precipitate and a brown solution of unknown composition were obtained; the precipitate was separated by filtration and washed with acetone and CH_2Cl_2. Yield: 30%. Anal. Calcd (found) for $C_{32}H_{36}N_6O_8Ru_2$: C, 46.02 (46.15); H, 4.31 (4.51); N, 10.06 (9.94). UV ($CHCl_3$) λ_{max}, nm (ϵ, M^{-1} cm^{-1}): 700 (22000). UV λ_{max}, nm: CH_2Cl_2, 705; CH_3CN, 707; DMF, 711; DMSO, 714. ^1H NMR (300 MHz, $CDCl_3$): δ 1.88 (s, 6H, acac CH_3), 1.90 (s, 6H, acac CH_3), 2.18 (s, 6H, acac CH_3), 2.34 (s, 6H, acac CH_3), 5.22 (s, 2H, acac CH), 5.38 (s, 2H, acac CH), 8.38 (m, 2H, bptz), 7.57 (m, 1H, bptz), 7.26 (m, 1H, bptz, overlaps with chloroform residual). FAB+ MS (nitrobenzyl alcohol matrix) *m*/*z*, obs (calc): 836 (836, M^+), 737 (737, $(M\text{-acac})^+$).

Preparation of $[Ru_2(acac)_4(bptz)](PF_6)$ (II). To **I** (50 mg, 0.06 mmol) in 20 mL of methanol was added cerium(IV) ammonium nitrate (33 mg, 0.06 mmol) in methanol (10 mL), which resulted in an immediate color change from green to blue. The reaction mixture was stirred at 25 °C for 1 h, and then the solution was concentrated by evaporation to about 5 mL, and **II** was precipitated by the addition of a saturated solution of NH_4PF_6 in water. UV λ_{max}, nm: CH_2Cl_2, 579; $CHCl_3$, 579; CH_3CN, 575; DMF, 586; DMSO, 583. Anal. Calcd (found) for $C_{32}F_6H_{36}N_6O_8PRu_2$: C, 39.2 (41.43); H, 3.67 (4.68); N, 8.58 (6.75). FAB^+ MS (nitrobenzyl alcohol matrix) *m*/*z*, obs (calc): 836 (836, $(M\text{-}PF_6)^+$), 737 (737, $(M\text{-}PF_6\text{-}acac)^+$). EPR data: Isotropic signal (g = 2.17) in CH_3CN glass at 77 K and 4 K. IR (thin film on KBr plate), energy in cm^{-1} (rel intensity): 559 (27), 842.5 (100), 1016 (28), 1264 (16), 1368 (27), 1425 (27), 1518 (92), 1550 (40), 2916 (24). Near-IR solvent, λ_{max}, nm, (ϵ, M^{-1} cm^{-1}): CH_2Cl_2, 1217 (20); CH_3CN, 1238 (20); $CHCl_3$, 1219 (12).

Results

Synthesis and Spectroscopic Properties of Complex I: Reaction of the orange−yellow *cis*-$Ru(acac)_2(CH_3CN)_2$ with dark fuscia bptz (2:1 molar ratio) in acetone under anaerobic conditions gives a green precipitate of complex **I** in 30% yield. Complex **I** is soluble in $CHCl_3$, moderately soluble in CH_2Cl_2, sparingly soluble in acetonitrile, DMF, DMSO, and methanol, and insoluble in alkanes. The bulk purity of the complex is demonstrated by the satisfactory elemental analysis and the absence of stray peaks in the NMR. Although the solid is air stable for months, partial air oxidation of a solution of **I** occurs over a period of hours and results in shifting and broadening of the NMR peaks due to the presence of paramagnetic Ru(III). The dimeric structure of **I** was confirmed by FAB+ mass spectroscopy. The agreement between the observed and calculated isotope pattern is excellent. The observed FAB signals are centered at *m*/*z* values of 836 and 737 amu, which correspond to $[\mathbf{I}]^+$ and $[\mathbf{I}\text{-acac}]^+$, respectively. Spectroscopic and electrochemical data for **I**, as well as a comparison with similar diruthenium complexes, is given in Table 1.

Each metal center in the dimer **I** could have either a Δ or Λ configuration of its three bidentate ligands. If these are formed randomly, then the synthesis ought to produce a pair of enantiomers and a meso compound. Kaim et al. observed both Δ, Δ and Λ, Λ enantiomers, and the *meso* compound in a synthesis of a related dimer.[12] However, for the isolated complex **I** we see only one set of NMR peaks, indicating that only one of the possible stereoisomers is isolated. Although these NMR data cannot distinguish between the C_s symmetric *meso* complex and an equimolar mixture of the C_2-symmetric enantiomers, X-ray crystallographic information (see below) shows that the preferred stereochemistry is the C_s symmetric Δ, Λ configuration (the *meso* complex). In view of the low isolated yield (30%) of **I**, it is possible that the other isomers may also be formed, but not isolated.

Electrochemical Properties of I. Complex **I** exhibits two reversible one-electron oxidation processes in CH_2Cl_2−0.1 M

(12) (a) Ernst, S.; Kasack, V.; Kaim, W. *Inorg. Chem.* **1988**, *27*, 1146. (b) Ernst, S. D.; Kaim, W. *Inorg. Chem.* **1989**, *28*, 1520.

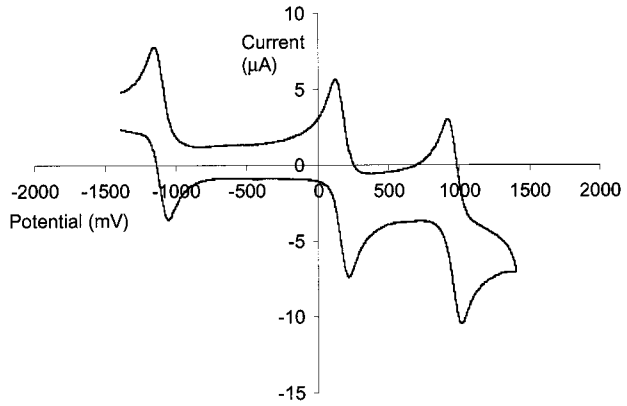

Figure 1. Cyclic voltammogram of $[Ru_2(acac)_4(bptz)]$ (**I**) in 0.1 M $TBABF_4$. Pt working and counter electrodes, Ag/AgCl reference, 100 mV/s scan rate.

$TBABF_4$; the cyclic voltammogram is shown in Figure 1. The oxidations at 0.17 and 0.97 V correspond to the couples $[\mathbf{I}]^{0}-[\mathbf{I}]^{1+}$ and $[\mathbf{I}]^{1+}-[\mathbf{I}]^{2+}$, respectively. The i_{pa}/i_{pc} ratios of unity and ΔE_p values of 60−70 mV at $\nu = 20-200$ mV s^{-1} indicate the reversibility of the processes. The 800 mV separation of these redox processes corresponds to a comproportionation constant of 10^{13}. The redox processes of **I** are greatly shifted from the potentials observed in multiply charged bptz dimers since it is easier to remove an electron from a neutral species than from a cationic species; the analogous couples in the complex $[Ru_2(NH_3)_8(bptz)]^{4+}$ occur at 0.72 and 1.56 V.

A reversible reduction is also observed at −1.11 V (ΔE_p = 80 mV); this reduction is assigned to the coordinated bptz ligand. Free bptz undergoes reduction at a potential of −0.77 V (ΔE_p = 140 mV) in the same electrolyte.

Molecular Structure of $\mathbf{I}\cdot 2CH_2Cl_2$. The structure of $\mathbf{I}\cdot 2CH_2Cl_2$ has been determined using single-crystal X-ray crystallographic methods.[13] The thermal ellipsoid plot of the complex $\mathbf{I}\cdot 2CH_2Cl_2$ is given in Figure 2, important bond distances and angles are shown in Table 2, and crystallographic data are given in Table 3. The two ruthenium atoms are in a distorted

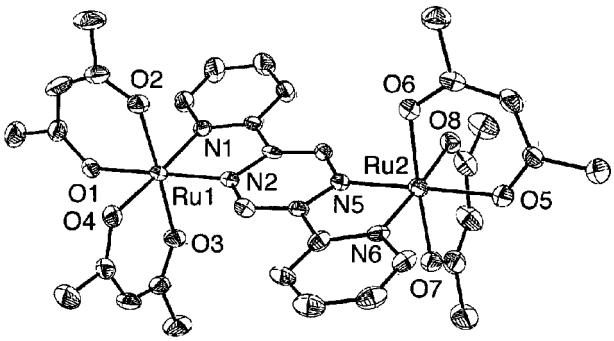

Figure 2. Thermal ellipsoid plot for $[Ru_2(acac)_4(bptz)]\cdot 2CH_2Cl_2$ (solvent omitted).

Table 2. Selected Bond Lengths (Å) and Angles (Deg) for $\mathbf{I}\cdot 2CH_2Cl_2$

Ru1−N2	1.946(6)	N1−Ru1−O4	174.0(2)
Ru1−O3	2.017(5)	O2−Ru1−O4	86.2(2)
Ru1−N1	2.020(6)	N2−Ru1−O1	174.6(2)
Ru1−O2	2.027(6)	O3−Ru1−O1	86.0(2)
Ru1−O4	2.052(5)	N1−Ru1−O1	95.1(2)
Ru1−O1	2.057(5)	O2−Ru1−O1	91.4(2)
Ru2−N5	1.943(6)	O4−Ru1−O1	87.7(2)
Ru2−N6	2.031(6)	N5−Ru2−N6	80.0(3)
Ru2−O6	2.033(5)	N5−Ru2−O6	88.8(2)
Ru2−O7	2.039(5)	N6−Ru2−O6	92.9(2)
Ru2−O8	2.043(5)	N5−Ru2−O7	94.4(2)
Ru2−O5	2.049(6)	N6−Ru2−O7	88.5(2)
Ru1−Ru2	6.9635(5)	O6−Ru2−O7	176.7(2)
N2−Ru1−O3	90.4(2)	N5−Ru2−O8	96.6(2)
N2−Ru1−N1	81.0(3)	N6−Ru2−O8	176.3(2)
O3−Ru1−N1	91.9(2)	O6−Ru2−O8	85.6(2)
N2−Ru1−O2	92.2(2)	O7−Ru2−O8	93.1(2)
O3−Ru1−O2	177.4(2)	N5−Ru2−O5	177.2(2)
N1−Ru1−O2	88.3(2)	N6−Ru2−O5	97.2(2)
N2−Ru1−O4	96.6(2)	O6−Ru2−O5	91.4(2)
O3−Ru1−O4	93.6(2)	O7−Ru2−O5	85.5(2)
		O8−Ru2−O5	86.2(2)

Table 3. Crystallographic Data for $[Ru_2(acac)_4(bptz)]\cdot 2CH_2Cl_2$

$C_{34}H_{40}N_6O_8Cl_{4.07}Ru_2$	fw = 1006.96 amu
$a = 11.709(2)$ Å	space group $P\bar{1}$
$b = 13.487(3)$ Å	$T = 290$ K
$c = 15.151(3)$ Å	λ (Mo Kα) = 0.7107 Å
$\alpha = 65.701(1)°$,	$\rho_{calcd} = 1.640$ g cm^{-1}
$\beta = 70.610(1)°$,	
$\gamma = 75.50(2)°$	
$V = 2038.8(6)$ Å^3	R indices ($I > 4\sigma I$): R1 = 0.0610, $wR_2 = 0.1334$
$Z = 2$	R indices (all data): R1 = 0.1169, wR_2 (all data) = 0.1633

octahedral geometry, and they lie in one plane with the bptz ligand; the bptz is not twisted or buckled. The Ru−O bonds *trans* to the strong π-acceptor bptz, eg. Ru1−O1 (2.057(5) Å), are longer than the ones *trans* to acac, such as Ru1−O3 (2.017(5) Å). The bonds from ruthenium to the pyridyl nitrogen atoms of the bptz are longer than the bonds from ruthenium to the tetrazine N atoms of the bptz, as previously observed in a bptz bridged dicopper complex.[6] Due to the chelating nature and π acidity of bptz, the Ru−N(pyridyl) bond lengths are shorter than those in 4,4′-bipy bridged diruthenium complexes.[14,15]

Synthesis and Spectroscopic Properties of Complex II. One-electron oxidation of **I** with Ce(IV) results in the quantita-

(13) (a) X-ray Crystallography of $\mathbf{I}\cdot 2CH_2Cl_2$. Dark green crystals of I were obtained by slow evaporation of solution of **I** in CH_2Cl_2. The crystals tended to deteriorate when mounted at the tip of a glass fiber, presumably due to loss of solvent of crystallization. A diamond shaped crystal of approximate dimensions 0.2 × 0.05 × 0.02 mm was mounted inside a capillary along with some mother liquor. Data were collected at 25 °C on an Enraf-Nonius CAD-4 diffractometer fitted with a graphite monochromated Mo Kα radiation source (λ = 0.71073 Å). The crystal orientation matrix and the unit cell parameters were derived from a least-squares fit to the goniometer settings of 25 reflections. The intensity data were collected in the θ limits 2.08−25.01 ($+h \pm k \pm l$) in the triclinic system. There were 7158 total reflections of which 4397 were observed with $F_o > 4\sigma(F_o)$. The data collected were corrected for Lorentz, polarization, and absorption effects using semiempirical factors based on ψ scans (transmission factors 0.568−0.647). Crystal quality was monitored by recording three standard reflections approximately every 160 reflections measured, and the decay was found to be negligible. The structure was solved by the Patterson method, and the space group was determined to be $P\bar{1}$ based on systematic absences. Ruthenium atoms were located on the Patterson map, and other non-hydrogen atoms were found on difference Fourier analysis. All non-hydrogen atoms were refined anisotropically. The hydrogen atoms were placed in calculated positions (riding model). There were additional peaks in the difference Fourier map, and these refined as carbons and chlorines of two disordered methylene chloride molecules. The site occupancy factor (s.o.f.) values for these atoms were refined, and the best s.o.f. was fixed during the least-square refinement. All calculations were done using SHELXTL (Bruker Analytical X-ray systems), with scattering factors and anomalous dispersions taken from the literature.[13b] (b) *International Tables of Crystallography*; Kluwer Academic Publishers: Dordrecht, The Netherlands, 1992; Vol. C.

(14) Szalda, D. J.; Fagalde, F.; Katz, N. E. *Acta Crystallogr.* **1996**, *C52*, 3013.

(15) Yan, H.; Suss-Fink, G.; Neels, A; Stoeckli-Evans, H. *J. Chem. Soc., Dalton Trans.* **1997**, 4345.

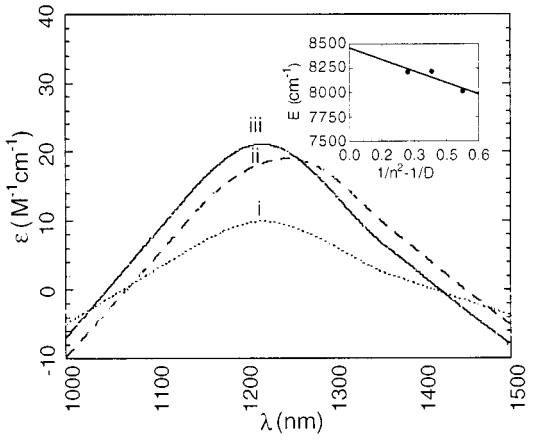

Figure 3. Near-IR bands of $[Ru_2(acac)_4(bptz)](PF_6)$ (**II**) in solvents (i) $CHCl_3$, (ii) CH_3CN, and (iii) CH_2Cl_2. Inset shows plot of E_{band} versus solvent polarity function.

tive formation of **II**. Complex **II** is insoluble in benzene and alkanes, but dissolves in chlorinated hydrocarbons, acetonitrile, and DMF. The FAB^+ mass spectrum of **II** was basically identical to that of **I**, showing peaks centered at *m*/*z* 836 amu $(\mathbf{II}\text{-}PF_6)^+$ and 737 amu $(\mathbf{II}\text{-}PF_6\text{-acac})^+$. The strong bands at 842.5 and 1500−1550 cm^{-1} in the IR spectrum of **II** are assigned as PF_6 and acac carbonyl stretches, respectively. In addition to a MLCT band at 575 nm in chloroform, complex **II** exhibits a very weak (ϵ, M^{-1} cm^{-1} ∼ 20) band at 1220 nm which we assign as the IVCT band. This NIR band was always observed against a large background absorbance, due to the tail from the very intense MLCT band. A linear background correction was used to subtract out this tail, giving the spectra shown in Figure 3.

Complex **II** is paramagnetic, as expected for an odd-electron species. Its EPR spectrum in frozen CH_3CN at 4 K is a broad, symmetrical S = 1/2 peak centered at a *g* value of 2.17. The closeness of the *g* value to the free electron value of 2 and the lack of observable parallel and perpendicular components implies that there is very little mixing of the ground-state orbital which holds the unpaired electron with other metal orbitals. Hyperfine splitting of the EPR spectrum is not observed for **II** even at 4K. Electrochemically generated $[Ru_2(NH_3)_8(bptz)]^{5+}$ in frozen acetonitrile and pyrazine-bridged Ru_2(II,III) species were found to show rhombic EPR spectral patterns.[16]

Discussion

Neutral complex **I** exhibits an intense charge-transfer band at 700 nm in chloroform (ϵ = 22,000 M^{-1} cm^{-1}), tailing off to the red, which is assigned as a Ru dπ−bptz pπ* charge transfer. The position of this band is not solvent sensitive. The aqueous solution of a related complex, $[Ru_2(NH_3)_8(bptz)]^{4+}$, exhibits a MLCT band at 603 nm (ϵ = 19,000 M^{-1} cm^{-1}).[6c] The 2440 cm^{-1} difference in MLCT energies can be ascribed to charge effects, which in the tetracation lower the energy of the Ru d orbitals relative to the bridge orbitals. The effect of adding 4 units of positive charge to a bptz-bridged dimer can thus be compared to the effect of an actual oxidation of the dimer, which in the case of complex **I** raises the MLCT energy by 3250 cm^{-1} to 575 nm (ϵ ∼ 13000 M^{-1} cm^{-1}).

To classify the mixed-valent complex **II** as partially or totally delocalized, the solvent effect on the 1220 nm band (assigned as an IVCT band) was studied in CH_2Cl_2, $CHCl_3$, and CH_3CN (Figure 3).[17] The polarities of these solvents are estimated by the solvent polarity function $1/n^2-1/D$, where *n* is the solvent's refractive index and *D* represents the dielectric constant.[17] A plot of the energy of the NIR transition in each of these solvents versus the solvent polarity function (see inset of Figure 3) gives a straight line with a slope of 780 and intercept of 8455 cm^{-1}. The intercept is interpreted as the Franck−Condon inner sphere optical activation energy. The NIR band maximum in complex **II** does not shift as a function of solvent polarity, which implies that the solvent reorganization for that electronic transition is negligible.[12,18] This casts complex **II** as a delocalized mixed-valence complex.

Weakly coupled and strongly coupled systems are predicted to give different line widths for the IVCT transition. This can be thought of as resulting from a transition from a relatively flat potential energy (PE) surface to a steep one in the weak coupling case (which produces a relatively broad absorbance peak) versus a transition from a flat PE surface to another flat PE surface in the strong coupling case (which produces a narrow absorbance peak). In the weak coupling limit, Hush's formula[17] (eq 1 below) predicts a line width of 4350 cm^{-1} for complex **II**.

$$\Delta\nu_{1/2}\,(\mathrm{cm}^{-1}) = (2310\nu_{\max})^{1/2} \qquad (1)$$

The experimental line widths in different solvents varied from 1980 to 2300 cm^{-1}, values that are too small to correspond to weak coupling. These observations suggest that **II** is a delocalized (Class III) system.

Acknowledgment. We are grateful for the support from ONR/DARPA Grant No. N00014-99-1-0472 which enabled us to begin investigating this class of mixed-valence compounds. We thank our colleague Dr. Robert Scheidt for providing his NIR spectrometer, Dr. Joseph Bularzik for help with the EPR measurements, and Dr. Robert Hayes for sharing his insights on EPR.

Supporting Information Available: X-ray crystallographic file in CIF format including atomic coordinates, thermal parameters, complete listings of bond distances and angles. This material is available free of charge via the Internet at http://www.acs.org.

IC001374W

(16) (a) Poppe, J.; Moscherosch, M.; Kaim, W. *Inorg. Chem.* **1993**, *32*, 2640. (b) Hush, N. S.; Edgar, A.; Beattie, J. K. *Chem. Phys. Lett.* **1980**, *69*, 128.

(17) (a) Hush, N. S. *Prog. Inorg. Chem.* **1967**, *8*, 391. (b) Hush, N. S. *Electrochim. Acta* **1968**, *13*, 1005.

(18) (a) Tom, G. M.; Creutz, C.; Taube, H. *J. Am. Chem. Soc.* **1974**, *96*, 7827. (b) Creutz, C. *Inorg Chem.* **1978**, *17*, 3725. (d) Tom, G. M.; Creutz, C.; Taube, H. *J. Am. Chem. Soc.* **1974**, *96*, 7829.